Synthesis and Characterization of Controlled Size CdSe Quantum Dots by Colloidal Method

Ganesh R. Bhand[1], Manorama G. Lakhe[1], Ashwini B. Rohom[1], Priyanka U. Londhe[1],
Sulabha K. Kulkarni[2], and Nandu B. Chaure[1, *]

[1] Department of Physics, Savitribai Phule Pune University, Pune 411007, India
[2] Department of Physics, Indian Institute of Science Education and Research, Dr. Homi Bhaba Road, Pune 411008, India

Monodispersed and highly luminescence cadmium selenide (CdSe) quantum dots (QDs) have been prepared in a single pot by colloidal reaction method. The QDs were characterized using X-ray diffraction (XRD), Raman Spectroscopy, transmission electron microscope (TEM), energy dispersive spectroscopy (EDS), UV-visible absorption spectroscopy and photoluminescence (PL) spectroscopy to study the structural, morphological, compositional and optical properties. The growth temperature played an important role to control the particle size. The optical wavelength was found to be shifted systematically from 460 nm to 575 nm upon increasing the reaction temperature from 110 °C to 260 °C. The size of CdSe QDs, ∼2–4 nm was estimated from absorption data. The emission tail exhibited at higher wavelength in PL measurement for the QDs synthesized for lower reaction temperature revealed the presence of surface trap-states. A cubic crystal structure of CdSe QDs was revealed by XRD analysis. The spherical QDs of size 2 to 4.5 nm were observed from TEM analysis for the samples prepared at 140 °C, 200 °C and 260 °C. The sizes of QDs obtained by TEM are in good agreement with the results obtained from optical and XRD data. High resolution transmission electron microscopy (HRTEM) confirmed the cubic crystal structure of CdSe QDs. The Selected area diffraction (SAD) pattern exhibited diffused ring corresponds to (111), (220) and (311) reflections of cubic structure of CdSe. The compositional analysis studied by EDS revealed the growth of nearly stoichiometric CdSe QDs. The LO1 vibrational mode observed about 202–205 cm^{-1} decreases the broadening systematically upon increasing the reaction temperature.

Keywords: CdSe QDs, X-ray Diffraction, TEM, Photoluminescence, Raman Spectroscopy.

1. INTRODUCTION

The colloidal synthesis of II–VI and III–V semiconductor nanocrystal are of great interest owing to their tunable electronic and optical properties for potential applications in optoelectronic devices.[1, 2] Photocatylysis,[3] solar energy conversion,[4] thin film transistor,[5, 6] and biomedical imaging.[7, 8] The optical, electrical and structural properties of semiconductor can be tailored by changing the size and shape of QDs. The synthesis of controlled size QDs within a narrow size distribution depends on the selection of solvent, capping ligands and growth temperature, etc. Cadmium selenide (CdSe) is II–VI semiconductor of direct band gap ∼1.74 eV at room temperature. When the crystallite size is less than Bohr radius, the quantum confinement effect becomes visible and its optical

spectrum can be shifted towards lower wavelength. Several methods have been developed to prepare semiconductor nanocrystals such as, hot injection method,[9] colloidal method,[10–13] micro-wave synthetic route,[14] green chemical approach,[15] solvothermal/hydrothermal route,[16, 17] and template assisted techniques.[18] Among above methods a colloidal method has been widely used to prepare the metal and semiconductor QDs with narrow size distribution. The different capping agents polyvinyl alcohol (PVA),[19] trioctylphosphine oxide (TOPO),[20] oleic acid (OA),[21, 22] were used to prepare the CdSe QDs by colloidal method. The size and shape dependent electrical and optical properties have been studied by numerous research groups.[22–24]

In a colloidal route, organometallic precursor dimethyl cadmium (Cd(CH$_3$)$_2$) is generally used for initial nucleation. The synthesis involves high-temperature

---

decomposition of $Cd(CH_3)_2$, which react with the solvent and process may become uncontrollable. Further, $Cd(CH_3)_2$ is extremely hazardous, expensive, pyrophoric, air-sensitive, and explosive at elevated temperature.[25, 26] Therefore, for large scale synthesis $Cd(CH_3)_2$ is not suitable. The nonpyrophoric, environmental and user friendly reactants such as CdO or $Cd(Ac)_2$ are more favorable for the large scale synthesis of high quality CdSe QDs.[27, 28] Oleic acid is relatively less expensive than that of the hexylphosphonic acid (HPA) and tetradecylphosphonic acid (TDPA) and can also act as solvent as well as capping ligand.[29–31] We have used trioctylphosphine oxide to stabilize the QDs as well as to protect the agglomeration of QDs.

2. EXPERIMENTAL DETAILS

2.1. Materials

Cadmium oxide (CdO) (99.99%), selenium (Se) powder (99.5%), trioctylphopsphine oxide (TOPO) and trioctylphosphine (TOP) (analytical grade, 95%), chloroform, methanol and oleic acid (OA) were purchased from Sigma Aldrich. All chemicals and solvents were used as received.

2.2. Synthesis of CdSe QDs

The solution of selenium (Se) and cadmium (Cd) precursor was prepared separately with two different processes. Firstly, the Se precursor was prepared with 0.6 mM of Se powder and TOP. The mixture was sonicated at room temperature for few minutes to get the clear solution. Secondly, the matrix consisting 0.3 mM CdO and oleic acid was prepared ~250 °C under nitrogen ambient. 0.3 mM TOPO was introduced into above solution at room temperature and heated up to 100 °C. The TOP-Se solution was rapidly injected into the above solution to start nucleation (reaction). The temperature of the final product was increased up to 260 °C with rate 1 °C/min. At different temperature (i.e., 110 °C, 140 °C, 170 °C, 200 °C, 230 °C and 260 °C), an aliquot of 1 ml was removed from reaction mixture and diluted in 5 ml chloroform solution to quench the further growth of QDs. The final product was centrifuged ~10 K rpm for several times with methanol and chloroform to remove the byproducts and impurities. The optical properties of the final solution were studied by using UV-vis spectrophotometer (model JASCO V-670) and photoluminescence spectrometer (model Perkin Elmer LS-55). The structural properties of sample collected by centrifugation process were studied by X-ray diffractometer (model D8 ADVANCED Burker) with CuKα radiation of wavelength $\lambda = 0.154$ nm. The size of the QDs was imaged by TEM model TECNAI G^2 with an accelerating voltage 200 kV. The inter planer distance and the presence of reflections was studied by HRTEM and selected area diffraction (SAD) pattern. The Energy Dispersive Spectroscopy (EDS) was performed using above

TEM instrument. The Raman spectroscopy was performed by INVIA RENISHAW Raman micrometer with Ar laser of wavelength 532 nm.

3. RESULTS AND DISCUSSION

3.1. X-ray Diffraction Analysis

Figure 1 shows the XRD spectrum of CdSe QDs prepared for various reaction temperatures between 110 °C to 260 °C. Three prominent peaks attributed to $2\theta = 25.30°$, 42.04° and 49.74° correspond to (111), (220) and (311) reflections of CdSe cubic phase [JCPDS-19–0191]. Sharp peaks exhibited in Figure 1(a) are associated to the elemental Se marked as solid circles (•). The presence of elemental Se peaks could be due to the incomplete reaction at low reaction temperature. The Se peaks were reduced for the sample prepared to 140 °C (Fig. 1(b)). The reaction temperature above 170 °C was found to be suitable for the synthesis of CdSe QDs is shown in Figures 1(c)–(f). The broad appearance of the reflections is associated to the synthesis of QDs. The average crystallite size was calculated for the highest intensity (111) peak by using the Scherrer's formula, which was found to be increased systematically from 1.60 to 2.98 nm upon increasing the growth temperature. The calculated values of crystallite size tabulated in Table I are good agreement with the particle size obtained by TEM and optical studies.
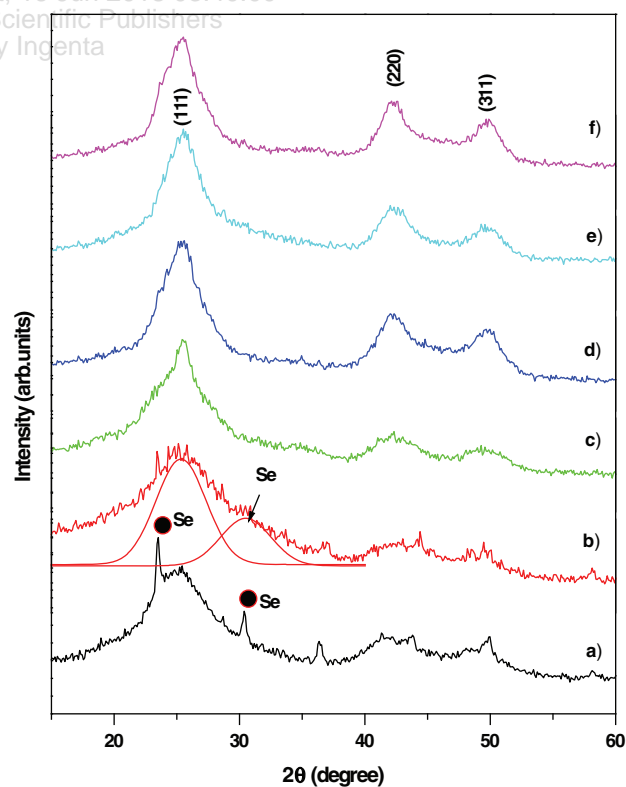
Figure 1. XRD spectra of CdSe QDs synthesized at reaction temperatures (a) 110 °C, (b) 140 °C, (c) 170 °C, (d) 200 °C, (e) 230 °C and (f) 260 °C.

Table I. A summary of band gap and particle size calculated from absorption and XRD results.

Growth temperature of CdSe QDs (°C)	Band gap estimated from optical measurements (eV)	Calculated particle size		FWHM of (111) peak (radian)
		Optical spectra (nm)	Scherrer formula (nm)	
110	2.52	2.02	1.60	5.13
140	2.44	2.08	1.95	4.88
170	2.28	2.27	2.65	3.14
200	2.19	2.53	2.88	2.89
230	2.12	2.98	2.94	2.85
260	2.02	3.87	2.98	2.79

3.2. Transmission Electron Microscopy (TEM) Studies

The size of the QDs and crystalline properties were studied by TEM analysis. The TEM images of CdSe QDs prepared at reaction temperatures 140 °C, 200 °C and 260 °C are shown in Figures 2(a)–(c), respectively. The resulting QDs of the sample prepared at 140 °C were small of an average size 1.5–2 nm, whereas, the samples prepared at 200 °C and 260 °C shows narrow size distributed spherical particles of an average size ∼3 and 4.5 nm, respectively. The value of the interplaner distance, $d \sim 3.51$ Å

to 3.52 Å was obtained from HRTEM, which is the lattice spacing for (111) plane of cubic crystal structure of CdSe. The selected area diffraction (SAD) pattern show a set of broad diffused rings along with spots due to the random orientation of the crystallites corresponding to diffraction from different planes of the QDs. The SAD pattern of CdSe prepared at lower temperature (140 °C) observed the spotty ring corresponds to the (202), (221) and (013) planes of elemental monoclinic [JCPDS-73–2121] Se and diffused rings are corresponds to (111), (220) and (311) planes of cubic CdSe. The sample prepared at 200 °C and 260 °C, exhibit only three diffused rings corresponds to (111), (220) and (311) reflections of cubic CdSe. The HRTEM and SAD images are given adjacent to each TEM image of the sample.

The compositional analysis obtained by EDS technique of the QDs prepared at 140 °C, 200 °C and 260 °C is shown in Figure 3. The QDs prepared at lower temperature (140 °C) were Se-rich and the contents of Se were found to be systematically decreased upon increasing the reaction temperature. This is in good agreement with XRD results discussed in previous section. The elemental atomic percentage concentration obtained from EDS analysis is tabulated in Table II. The ratio of Cd/Se was found nearly
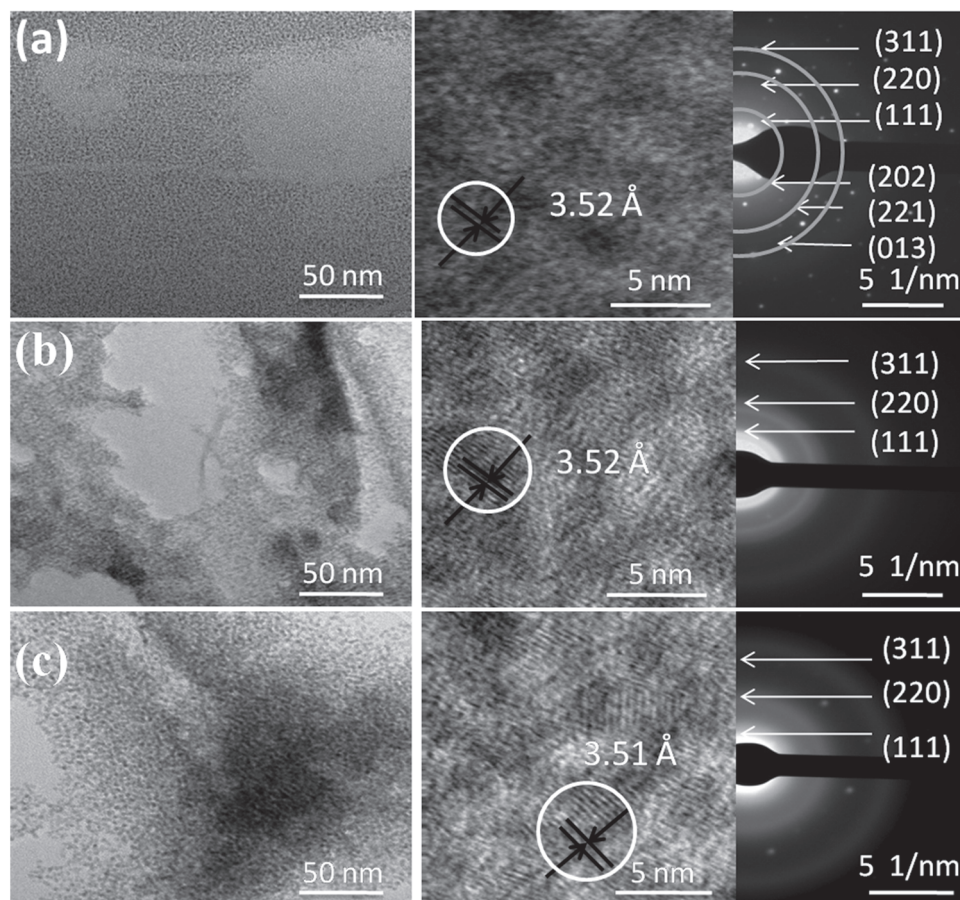
Figure 2. TEM image of the CdSe QDs prepared at temperature (a) 140 °C, (b) 200 °C and (c) 260 °C. The corresponding images are HRTEM and SAD pattern, respectively.
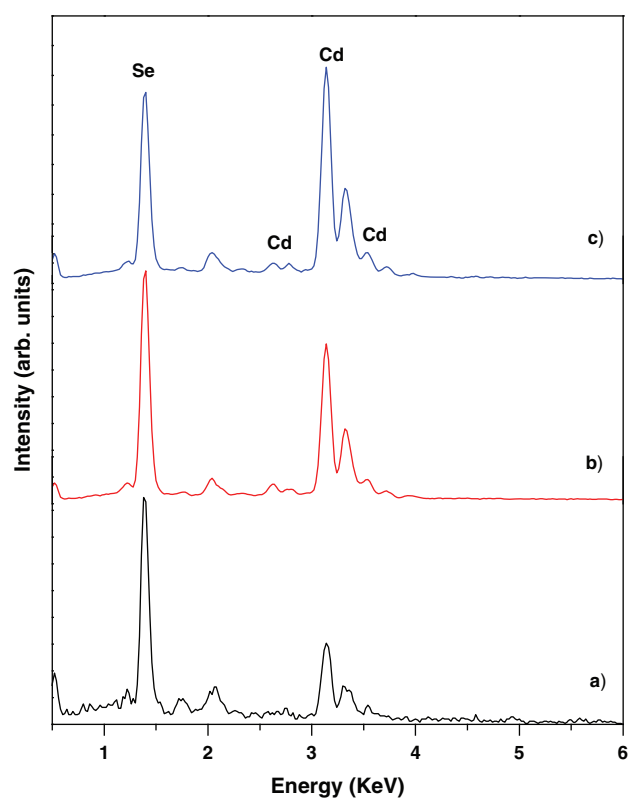
Figure 3. EDS spectra of the sample prepared at (a) 140 °C, (b) 200 °C and (c) 260 °C.

unity for the QDs prepared at higher (260 °C) reaction temperature.

3.3. Absorption Studies

The optical absorption spectrum of CdSe QDs prepared for different temperatures is shown in Figure 4(A). The QDs prepared at 110 °C, 140 °C, 170 °C, 200 °C, 230 °C and 260 °C exhibited a absorption peaks at 460 nm, 469 nm, 492 nm, 518 nm, 542 nm and 575 nm, respectively. The absorption peak attributed on each curve indicates the formation of QDs. The peak position of CdSe QDs recorded in the absorption spectra was found to be red shifted systematically from 460 nm to 575 nm upon increasing the reaction temperature, which is associated to the size of QDs. The actual photograph of the CdSe QDs synthesized at various temperatures is shown in inset of Figure 4(A). The change in the solution of color is due to the synthesis of different size QDs.

Table II. A summary of elemental composition of CdSe QDs obtained by EDS analysis.

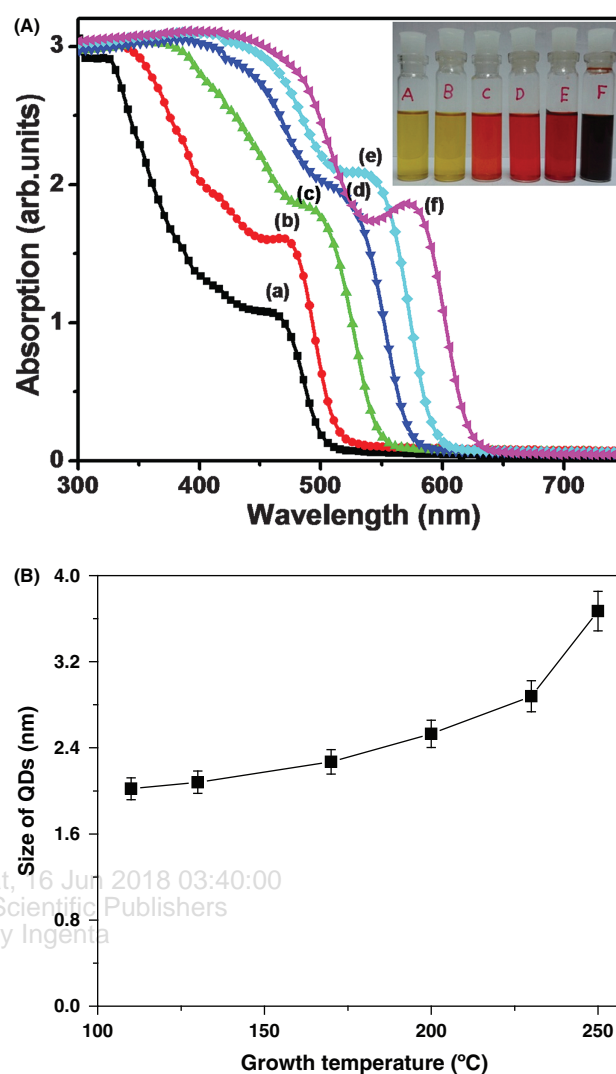| Growth temperature of CdSe QDs (°C)	Atomic percentage concentration		
	Cd	Se	Cd/Se
140	45.03	54.97	0.82
200	47.77	52.23	0.91
260	50.82	49.18	1.03

Figure 4. UV-Vis absorption spectra and the actual photograph of the prepared CdSe QDs are represented in the inset (A) and plot of variation of average particle size as a function of reaction temperature (B).

The average size of the CdSe QDs was calculated from absorbance spectra, using the relation,[32]

$$D = (1.6122 \times 10^{-9})\lambda^4 - (2.6575 \times 10^{-6})\lambda^3$$
$$+ (1.6242 \times 10^{-3})\lambda^2 - (0.4277)\lambda + (41.57) \quad (1)$$

where 'D' is the average diameter of CdSe QDs, and 'λ' is wavelength of excitonic absorption peak of corresponding sample. The calculated values of QDs are close to the results obtained by TEM and XRD data. The average particle size calculated from Eq. (1) is represented in Figure 4(B).

The optical transition energy (E_g) has been calculated from absorption coefficient data by using Tauc's relation.[33]

$$(\alpha h\nu) = A(h\nu - E_g)^n \quad (2)$$

where 'α' is the absorption coefficient, '$h\nu$' is the photon energy, 'A' is constant, 'E_g' is the energy band gap of

CdSe QDs grown at different reaction temperature, and 'n' assume the values 1/2, 2, 3/2, and 3 for allowed direct, allowed indirect, forbidden direct and forbidden indirect transitions, respectively. It is well known that CdSe is a direct band gap semiconductor; therefore, the value of n has taken to be 1/2 in above equation.

Figure 5 shows the plot of $(\alpha h\nu)^2$ versus $(h\nu)$ for the CdSe samples prepared at different reaction temperatures. The straight line nature of the plots over a wide range of photon energy indicates the direct transition in the material. The optical transition energy has been determined by the extrapolation of the straight line portion on the energy axis at $(\alpha h\nu)^2 = 0$. The estimated value of optical transition energies for CdSe QDs prepared at temperatures 110 °C, 140 °C, 170 °C, 200 °C, 230 °C and 260 °C are 2.52, 2.44, 2.28, 2.19, 2.12 and 2.02 eV, respectively. Note that these values are much larger than the energy band gap of bulk CdSe.

We have further used effective mass approximation,[33] to estimate the particle size from optical data.

$$E_g = E_g^{bulk} + \frac{h^2\pi^2}{2R^2}\left(\frac{1}{m_e^*} + \frac{1}{m_h^*}\right) - \frac{1.8e^2}{4\pi\varepsilon\varepsilon_0 R} \qquad (3)$$

where, E_g is the optical transition energy of CdSe QDs which is estimated from the optical absorption spectra, E_g^{bulk} is the energy gap of the bulk semiconductor (1.74 eV for CdSe) and m_e^* and m_h^* are the effective masses of the conduction band electrons and the valence band holes of CdSe, respectively. The values of m_e^* and m_h^* for CdSe are 0.13 m_o and 0.45 m_o, m_o is the electron rest mass $(9.1 \times 10^{-31}$ kg), h is the Plank's constant, R is the radius of the QDs, ε is the dielectric constant of the material (for CdSe, $\varepsilon = 10.2$),[19] and ε_0 is the permittivity of free space. The estimated sizes from Eq. (3) for CdSe QDs grown at temperature of 110 °C, 140 °C, 170 °C, 200 °C, 230 °C and 260 °C was 2.10, 2.45, 3.22, 3.72, 4.20 and 4.50 nm,
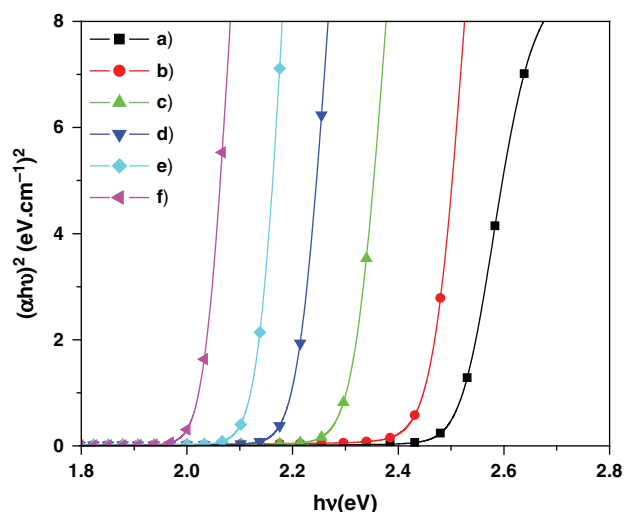
respectively, which agrees well with result obtained by other measurement techniques.

3.4. Photoluminescence (PL) Measurement

Figure 6 shows the PL spectra of CdSe QDs prepared at different reaction temperatures. A clear red-shift in the band edge emission peak is observed for the QDs prepared for lower to higher reaction temperatures, which is associated to the size of QDs. The PL spectra of CdSe QDs prepared at lower reaction temperatures 110 °C and 140 °C reveals a band-edge emission with FWHM 45 nm and 43 nm, respectively and a broad tail at higher wavelength may be due to the surface-trap state present in the material,[15] or related to the presence of excess elemental selenium. On the other hand, the CdSe QDs prepared at higher reaction temperatures (170 °C, 200 °C, 230 °C and 260 °C) shows only a sharp band-edge emission in red spectral region with FWHM between 28 nm to 36 nm. The sharp and narrow excitonic absorption peaks in PL spectra suggest that the prepared CdSe QDs are reasonably mono-dispersed with narrow size distribution.

3.5. Raman Analysis

Raman spectra recorded to CdSe QDs prepared for reaction temperatures 140 °C, 200 °C and 260 °C are shown in Figure 7. The high intensity LO1 peak associated to Se–Cd–Se symmetric vibration is exhibited several wavenumbers lower than that of the bulk CdSe.[34] The similar results are reported for CdSe QDs by Lu et al.[35] This shift is an indication of the phonon confinement effect in the present QDs. The shift in the peak position to lower wavelength could be also associated to superposition of smaller and larger QDs. The shoulder observed around 406–409 cm^{-1} is associated to the overtone (LO2) of LO1 peak. The broadening of the LO1 mode decreases systematically upon increasing the reaction temperature. The FWHM was
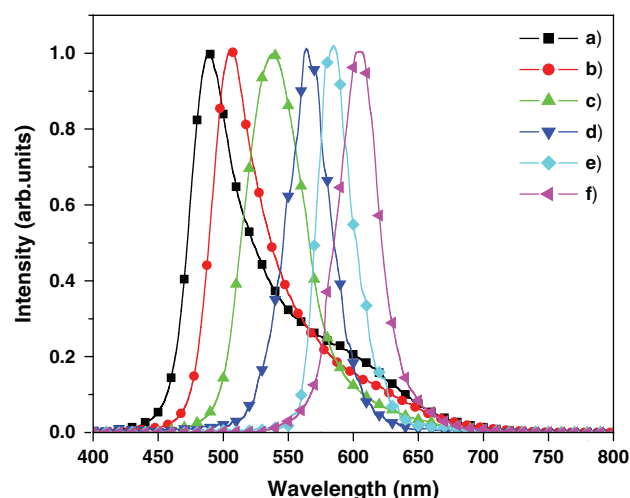
Figure 5. $(\alpha h\nu)^2$ versus $(h\nu)$ plot of CdSe QDs prepared at different reaction temperatures.

Figure 6. Photoluminescence spectra of CdSe QDs prepared at different reaction temperatures.
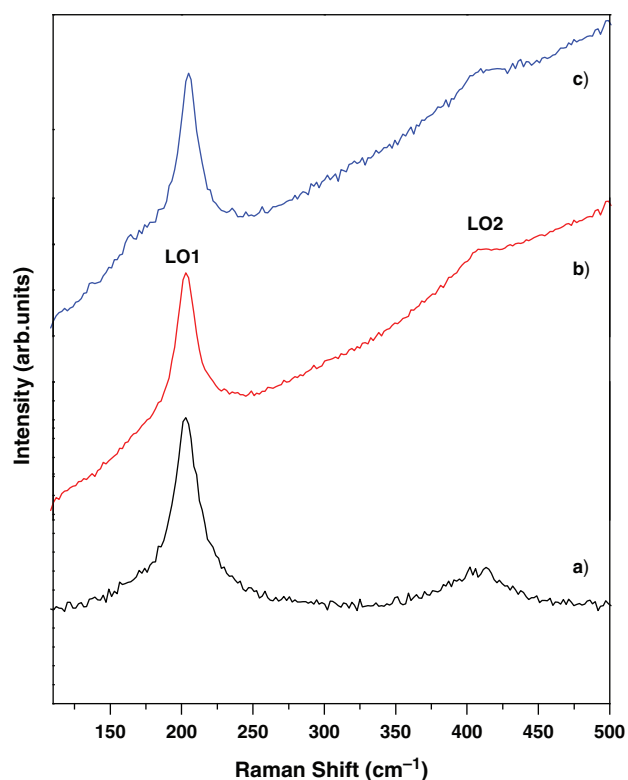
Figure 7. Raman spectra of CdSe QDs prepared at reaction temperatures (a) 140 °C, (b) 200 °C and (c) 260 °C.

measured ~20, 16 and 12 cm^{-1} for CdSe QDs prepared at 140, 200 and 260 °C, respectively. The broadening in the Raman peak with decrease in QDs size could be associated to the structural disorder.[36]

4. CONCLUSION

Uniform, spherical, narrow size distributed CdSe QDs have been prepared by simple colloidal reaction method. Reaction temperature affects significantly on the size of QDs. The optical and structural data revealed that the particle size increases upon increasing the reaction temperature. The systematic red shift revealed in the optical spectra is due to the systematic change in QDs. The optical energy band gap has been estimated from absorption data in the range 2 to 2.52 eV. The emission tail observed at higher wavelength in PL measurement associated to the presence of surface trap-states. XRD analysis confirms the cubic structure of CdSe QDs. Nearly stoichiometric CdSe QDs have been prepared at higher growth temperature (260 °C). The SAD pattern exhibit diffused rings corresponds to (111), (220) and (311) reflections of cubic structure of CdSe. The longitudinal optical phonon, LO1 and its first overtone, LO2 are exhibited at ~204 cm^{-1} and ~407 cm^{-1}, respectively.

References and Notes

1. J. Song, J. Li, X. Li, L. Xu, Y. Dong, and H. Zeng, *Adv. Mater.* 27, 7162 (**2015**).
2. Z. Yuan, M. Fu, Y. Ren, W. Huang, and C. Shuai, *Microelectron. Eng.* 163, 32 (**2016**).
3. A. Ayyaswamy, S. Ganapathy, A. Alsalme, A. Alghamdi, and J. Ramasamy, *Superlattices Microstruct.* 88, 634 (**2015**).
4. U. Jabeen, S. M. Shah, N. Hussain, F. Alam, and A. Ali, *J. Photo-chemistry and Photobiology A: Chemistry* 325, 29 (**2016**).
5. P. P. Puczkarski, P. Gehring, C. S. Lau, J. Liu, A. Ardavan, J. H. Warner, G. Briggs, and J. A. Mol, *Appied Physics Letter* 107, 133105 (**2015**).
6. F. F. Vidor, T. Meyers, G. I. Wirthb, and U. Hilleringmann, *Micro-electron. Eng.* 159, 155 (**2016**).
7. A. Valizadeh, H. Mikaeili, M. Samiei, S. M. Farkhani, N. Zarghami, M. Kouhi, A. Akbarzadeh, and S. Davaran, *Nanoscale Research Letters* 7, 480 (**2012**).
8. S. J. Rosenthal, J. C. Chang, O. Kovtun, J. R. McBride, and I. D. Tomlinson, *Chemistry and Biology* 18, 10 (**2011**).
9. D. S. Wang, W. Zheng, C. H. Hao, Q. Peng, and Y. D. Li, *Chem. Eur. J.* 15, 1870 (**2009**).
10. R. K. Ratnesh and M. S. Mehata, *AIP Advances* 5, 097114 (**2015**).
11. S. Chaure, N. B. Chaure, and R. K. Pandey, *J. Nanosci. Nanotechnol.* 6, 731 (**2006**).
12. W. Vogel, J. Urban, M. Kundu, and S. K. Kulkarni, *Langmuir.* 13, 827 (**1997**).
13. G. R. Bhand, P. U. Londhe, A. B. Rohom, and N. B. Chaure, *Advance Science Letter* 20, 1112 (**2014**).
14. Z. K. Xu, F. Gao, Q. X. Wang, Z. S. Hu, and X. Fu, *J. Dispersion Sci. Technol.* 30, 365 (**2009**).
15. A. L. Washington and G. F. Strouse, *Chem. Mater.* 21, 3586 (**2009**).
16. Q. Wang, D. Pan, S. Jiang, X. Ji, L. An, and B. Jiang, *J. Cryst. Growth* 286, 83 (**2006**).
17. H. M. Wang, P. F. Fang, Z. Chen, and S. J. Wang, *J. Alloys Compd.* 461, 418 (**2008**).
18. X. S. Peng, J. Zhang, X. F. Wang, Y. W. Wang, L. X. Zhao, G. W. Meng, and L. D. Zhang, *Chemicals Physics Letters* 343, 470 (**2001**).
19. H. S. Mansur and A. A. P. Mansur, *Mater. Chem. Phys.* 125, 709 (**2011**).
20. C. A. Leatherdale, W. K. Woo, F. V. Mikulee, and M. G. Bawendi, *J. Phys. Chem. B* 106, 7619 (**2002**).
21. N. Li, X. Zhang, S. Chen, and X. Hou, *J. Phys. Chem. Solids* 72, 1195 (**2011**).
22. L. L. Han, D. H. Qin, X. Jiang, Y. S. Liu, L. Wang, J. W. Chen, and Y. Cao, *Nanotechnology* 17, 4736 (**2006**).
23. L. Manna, E. C. Scher, and A. P. Alivisatos, *Journal of American Chemical Society* 122, 12700 (**2000**).
24. S. N. Sharma, Z. S. Pillai, and P. V. Kamat, *J. Phys. Chem. B* 107, 10088 (**2003**).
25. G. Konstantatos, I. Howard, A. Fischer, S. Hoogland, J. Clifford, E. Klem, L. Levina, and E. H. Sargent, *Nature* 442, 180 (**2006**).
26. Z. A. Peng and X. Peng, *Journal of American Chemical Society* 123, 183 (**2001**).
27. G. Zlateva, Z. Zhelev, R. Bakalova, and I. Kanno, *Inorg. Chem.* 46, 16 (**2007**).
28. L. Qu, Z. A. Peng, and X. Peng, *Nano Letter* 1, 333 (**2001**).
29. Y. A. Yang, H. M. Wu, K. R. Williams, and Y. C. Cao, *Angew. Chem. Int. Ed.* 44, 6712 (**2005**).
30. L. Liu, Z. Zhuang, T. Xie, Y. G. Wang, J. Li, Q. Peng, and Y. Li, *Journal of American Chemical Society* 131, 16423 (**2009**).

31. H. Lee, S. W. Yoon, J. P. Ahn, Y. D. Suh, J. S. Lee, H. Lim, and D. Kim, *Solar Energy Materials and Solar Cells* 93, 779 **(2009)**.

32. W. W. Yu, L. Qu, W. Guo, and X. Peng, *Chem. Mater.* 15, 2854 **(2003)**.

33. W. E. Mahmoud, A. M. Al-Amri, and S. J. Yaghmour, *Opt. Mater.* 34, 1082 **(2012)**.

34. N. Tschirner, H. Lange, A. Schliwa, A. Biermann, C. Thomsen, K. Lambert, R. Gomes, and Z. Hens, *Chem. Mater.* 24, 311 **(2012)**.

35. L. Lu, X. Xu, W. Liang, and H. Lu, *J. Phys.: Condens. Matter.* 19, 406221 **(2007)**.

36. V. M. Dzhagan, M. Y. Valakh, A. E. Raevskaya, A. L. Stroyuk, S. Y. Kuchmiy, and D. R. Zahn, *Nanotechnology* 19, 305707 **(2008)**.